THE JOURNAL OF BIOLOGICAL CHEMISTRY VOL. 283, NO. 45, pp. 30754–30765, November 7, 2008

RhoA GTPase and F-actin Dynamically Regulate the Permeability of Cx43-made Channels in Rat Cardiac Myocytes*

Received for publication, February 26, 2008, and in revised form, July 21, 2008 Published, JBC Papers in Press, July 29, 2008, DOI 10.1074/jbc.M801556200

Mickaël Derangeon[‡], Nicolas Bourmeyster[‡], Isabelle Plaisance[‡], Caroline Pinet-Charvet[‡], Qian Chen[‡], Fabien Duthe[‡], Michel R. Popoff[§], Denis Sarrouilhe[‡], and Jean-Claude Hervé[‡1]

From the [‡]Institut de Physiologie et Biologie Cellulaires, Université de Poitiers, CNRS 6187, 40 avenue du recteur Pineau, F-86022 Poitiers and [§]Unité des Bactéries Anaérobies et Toxines, Institut Pasteur, 25–28 rue du Dr Roux, F-75724 Paris Cédex 15, France

Gap junctions are clusters of transmembrane channels allowing a passive diffusion of ions and small molecules between adjacent cells. Connexin43, the main channel-forming protein expressed in ventricular myocytes, can associate with zonula occludens-1, a scaffolding protein linked to the actin cytoskeleton and to signal transduction molecules. The possible influence of Rho GTPases, major regulators of cellular junctions and of the actin cytoskeleton, in the modulation of gap junctional intercellular communication (GJIC) was examined. The activation of RhoA by cytoxic necrotizing factor 1 markedly enhanced GJIC, whereas its specific inhibition by the *Clostridium botulinum* C3 exoenzyme significantly reduced it. RhoA activity affects GJIC without major cellular redistribution of junctional plaques or changes in the Cx43 phosphorylation pattern. As these GTPases frequently act via the cortical cytoskeleton, the importance of F-actin in the modulation of GJIC was investigated by means of agents interfering with actin polymerization. Cytoskeleton stabilization by phalloidin slowed down the kinetics of channel rundown in the absence of ATP, whereas its disruption by cytochalasin D rapidly and markedly reduced GJIC despite ATP presence. Cytoskeleton stabilization by phalloidin markedly reduced the consequences of RhoA activation or inactivation. This mechanism appears to be the first described capable to both up- or down-regulate GJIC through RhoA activation or, conversely, inhibition. The inhibition of Rho downstream kinase effectors had no effect on GJIC. The present results provide further insight into the gating and regulation of junctional channels and identify a new downstream target for the small G-protein RhoA.

In animal tissues, most cells are connected via intercellular cytoplasmic channels clustered in plasma membrane spatial microdomains termed gap junctions, which allow neighbor cells to directly exchange ions and small molecules. Each channel results from the docking of two half-channels, or connexons, formed by the oligomerization of six protein subunits (connexins (Cxs))[2] around an aqueous pore. Cxs are homologous proteins encoded by a multigene family and are named according to their predicted molecular weight. Cx43, widely distributed in different cell types, is the main gap junction protein expressed in mammalian ventricular myocytes, although Cx40 and Cx45 have also been reported to be expressed (1).

In cardiac myocytes of newborn rat, the degree of cell-to-cell communication is closely regulated by the metabolic state of the preparation, which undergoes a complete interruption of the gap junctional communication when the ATP concentration is lowered (2–4). This permeability decline of junctional channels was interpreted as being due to the unbalanced activity of endogenous protein phosphatase(s) (3), particularly of protein phosphatase 1 (PP1; Ref. 4). In preliminary experiments, GTP was found to preserve the intercellular cytoplasmic continuity in the absence of ATP, suggesting either that it was used as co-substrate by the unidentified protein kinase (PK), which counterparts PP1 activity, or that it was acting via a guanosine triphosphatase (GTPase). These enzymes are molecular switches that control a wide variety of signal transduction pathways in all eukaryotic cells.

In mammals, the members of the Rho family of small GTPases represent a group of 23 gene products; the best characterized members are RhoA, Rac1, and Cdc42 (5). Rho GTPases are in particular known as key regulators of the actin cytoskeleton, but their ability to influence cell polarity, gene transcription, cell cycle progression, membrane transport pathways, and many enzyme activities is probably just as significant (for a review, see Ref. 6). These molecular switches cycle between an inactive (GDP-bound) state and an active (GTP-bound) state. The exchange of hydrolyzed GDP for GTP results in a conformational change, unmasking structural domains by which they bind to the effectors. They recognize their target protein in the Rho-GTP state and generate a response until GTP is hydrolyzed. In ventricular myocytes of newborn rat,

* This work was supported in part by grants from the European Community Research and Technological Development Action QLG1-CT-1999-00516. The costs of publication of this article were defrayed in part by the payment of page charges. This article must therefore be hereby marked "*advertisement*" in accordance with 18 U.S.C. Section 1734 solely to indicate this fact.

[1] To whom correspondence should be addressed: Inst. de Physiologie et Biologie Cellulaires, UMR CNRS 6187, 40 ave. du recteur Pineau, F-86022 Poitiers, France. Tel./Fax: 33-549-45-37-51; E-mail: Jean.Claude.Herve@univ-poitiers.fr.

[2] The abbreviations used are: Cx, connexin; ZO-1, zonula occludens-1; CNF, cytoxic necrotizing factor; GJIC, gap junctional intercellular communication; PP, protein phosphatase; PK, protein kinase; PKN, protein kinase novel; GTPase, guanosine triphosphatase; GJ, gap junction; TRITC, tetramethylrhodamine isothiocyanate; ROCK, Rho-associated coiled coil-containing kinase; CRIK, citron kinase; G_j, conductance; AMP-PNP, adenosine 5′-(β,γ-imino)triphosphate; FRAP, fluorescence recovery after photobleaching.

immunoblot analyses and immunostainings revealed that RhoA was present predominantly in the cytosolic fraction, whereas RhoB was undetectable (7).

The extreme carboxyl terminus of Cx43 was shown to interact with the second PDZ domain of zonula occludens-1 (ZO-1; Refs. 8 and 9). The latter is a member of a family of multidomain membrane proteins called membrane-associated guanylate kinase homologs (MAGUK proteins), that couple the extracellular environment to intracellular signaling pathways and to cytoskeleton. The basic core of MAGUK proteins consists of a PDZ domain (PSD-95/Dlg/ZO-1), a SH3 (Src homology 3) domain and a GUK (guanylate kinase) domain (10). ZO-1 might then stabilize GJs through actin filament anchoring. In cultured ventricular myocytes of newborn rat, the co-localization of ZO-1 with individual Cx43 GJ plaques is limited to about 27% overlap (11) with ZO-1 preferentially localized at the periphery of the plaques (11, 12), and ZO-1 was proposed to control the rate of channel accretion at GJ plaque perimeters (12). An increase in the Cx43/ZO-1 interaction was observed during the remodeling of gap junctions after enzymatic dissociation (13), suggesting a dynamic role for ZO-1 in gap junction turnover.

Many aspects of connexin function, for example intracellular cellular transport, junctional plaque assembly and stability, and channel conductivity, are finely tuned and likely involve proteins that bind to the cytoplasmic domains of connexins. However, little is known about such regulatory proteins. The present study was designed to assess the possible contribution of Rho GTPase in the regulation of GJIC between rat ventricular myocytes. Cardiac-specific inhibition and activation of RhoA signaling are indeed both known to result in alterations of cardiac rhythm and conduction, processes where GJIC is of fundamental importance.

EXPERIMENTAL PROCEDURES

Cell Preparation—Experiments were performed with ventricular cardiomyocytes obtained from neonatal (1–2-day old) rats as described previously (14) and cultured for 2 or 3 days. The spontaneous synchronized mechanical activity was used as evidence to avoid confusion with non-muscle cells.

Endogenous ADP-ribosylation in Cardiomyocytes—ADP-ribosylation was performed as described previously (15, 16). Cardiomyocytes were preincubated for 1–3 h at 37 °C with Ia-C3 (5 μg/ml) in the presence of Ib (molar ratio, 1:1). The cells were washed twice with phosphate-buffered saline and lysed with ADP-ribosylation buffer (20 mM HEPES, pH 8, 2.5 mM $MgCl_2$, 1 mM dithiothreitol, 1 mM ATP, 15 mM thymidine, 15 mM Isonicotinic acid) containing 1 μg/ml leupeptin, 1 μg/ml pepstatin, 1 mM phenylmethylsulfonyl fluoride (Roche Applied Science), and 0.5% (v/v) Triton X-100. Cell debris were removed by centrifugation, and the supernatant (50 μg of total protein) was ADP-ribosylated *in vitro* in a final volume of 20 μl of ADP-ribosylation buffer containing 3.5 μM [^{32}P]NAD (1000 Ci/mmol) and 10^{-7} M C3 for 1 h. The reaction was stopped by addition of 0.06 M Tris-HCl, pH 7.0, 15% (v/v) glycerol, 5% β-mercaptoethanol, 2.3% SDS, and 0.001% bromphenol blue. The proteins were separated using 12% PAGE-SDS, the gel was dried and submitted to autoradiography, and the radiolabeled C3 substrate was visualized as a 24-kDa protein.

Evaluation of the Strength of Cell-to-cell Communication—Gap junctional conductance was obtained from cell pairs using a double whole cell voltage clamp configuration as described previously (14). The junctional permeability for the diffusion of a fluorescent dye (6-carboxyfluorescein) was estimated by analyzing the fluorescence recovery after photobleaching (FRAP; Ref. 17) as described previously (18) by means of a spectral confocal microscope station, FV 1000, installed on an inverted microscope, IX-81 (Olympus, Tokyo, Japan). Briefly after photobleaching of the fluorescence of the selected cell, the fluorescence redistribution from the unbleached cells to the bleached cells is monitored as a function of time. The initial recovery of fluorescence in the bleached cells follows a monoexponential time course, and the relative permeability constant (k) of the exponential fluorescence recovery (the inverse value of the time constant) is determined using Equation 1,

$$(F_i - F_t)/(F_i - F_o) = e^{-kt} \quad \text{(Eq. 1)}$$

where F_i, F_o, and F_t are the integrated fluorescence intensities in the bleached cells before photobleaching, immediately after photobleaching, and at time t after photobleaching, respectively.

Antibodies—The monoclonal mouse anti-Cx43 purchased from BD Transduction Laboratories (Interchim, Montluçon, France) was used in Western blot experiments, immunoprecipitation, or for the immunostaining. The mouse monoclonal anti-ZO-1 antibody purchased from Zymed Laboratories Inc. (Clinisciences, Montrouge, France) was used in Western blot experiments and for the immunostaining in combination with the anti-Cx43 antibody produced in rabbit (Sigma). The mouse monoclonal anti-N-cadherin purchased from BD Transduction Laboratories was used for the immunostaining in combination with the anti-Cx43 antibody produced in rabbit and the phalloidin-TRITC (both from Sigma). The secondary antibodies Alexa Fluor 488 goat anti-rabbit IgG, Alexa Fluor 555 goat anti-mouse IgG, Alexa Fluor 488 goat anti-mouse, and Alexa Fluor 635 goat anti-rabbit were purchased from Molecular Probes (Invitrogen). The goat anti-mouse antibody alkaline phosphatase conjugate was purchased from Promega, and the polyclonal goat anti-mouse immunoglobulins/horseradish peroxidase was from Dako (DakoCytomation, Trappes, France).

Immunofluorescence—Aliquots of freshly isolated ventricular myocytes were cultured on glass plates. Cells were washed with phosphate-buffered saline to discard cell debris and fixed in paraformaldehyde (0.5% (v/v); 10 min). After fixation, cells were rinsed and incubated for 1 h with a blocking and permeabilizing solution (4% bovine serum albumin (w/v) and 0.5% Triton X-100 (v/v) in phosphate-buffered saline). Cells were then incubated directly with the needed antibody overnight at 4 °C in the same solution. After extensive washing, cells were incubated with the corresponding secondary antibody and TOPRO 3 (diluted 1:1000) to label cell nuclei or phalloidin-TRITC (diluted 1:100) to label actin in blocking solution for 45 min at room temperature (22–24 °C). Following the final rinse, the cells were mounted with a glass slide with fluorescence mounting medium (Vectashield, Vector Laboratories) and examined using the confocal microscope station. The images

show either separated red or green fluorescence or their combination (yellow).

Image Analysis—Cx43 individual plaque areas were evaluated by means of Image J software (National Institutes of Health). Briefly each image with Cx43 labeling was converted into a binary (*i.e.* black and white) image. The background for all photographs was similarly normalized (Image J automatic thresholding algorithms), and plaque areas were evaluated by means of Image J particle analysis algorithms (19).

Co-immunoprecipitation and Western Immunoblotting—Cardiomyocytes were preincubated for 3–6 h at 37 °C with Ia-C3 (5 μg/ml) in the presence of Ib (8 μg/ml) or with CNF (200 ng/ml). The cells were washed twice with phosphate-buffered saline and were harvested and homogenized in a buffer containing 1% Triton X-100, 100 mM NaCl, 1 mM EGTA, 50 mM Tris-HCl, pH 7.4, 1 mM Na_3VO_4, 50 mM NaF, 1 mM phenylmethylsulfonyl fluoride (Roche Applied Science), and protease inhibitor mixture (1:100 dilution; Sigma). Samples were homogenized, sonicated, and centrifuged at 14,000 $\times$ *g* for 15 min at 4 °C. Total homogenate protein was determined using the Bio-Rad DC assay kit. For immunoprecipitation, the cell lysate was precleared and incubated overnight at 4 °C with a monoclonal mouse anti-Cx43 from BD Transduction Laboratories. 40 μl of protein G-Sepharose (Amersham Biosciences) were then added for 1 h under agitation at 4 °C. After immunoprecipitation, bead-bound complexes were washed six times, collected, and resuspended in 20 μl of Laemmli buffer (20). Sodium dodecylsulfate-polyacrylamide gel (10%) electrophoresis for Cx43, gradient gel (4–12%) electrophoresis for ZO-1, and Western blotting on nitrocellulose membranes were performed. ZO-1 and Cx43 detection was carried out with the mouse monoclonal anti-ZO-1 antibody (Zymed Laboratories Inc.) or the mouse monoclonal anti-Cx43 antibody (BD Transduction Laboratories). To confirm reproducibility, all experiments were repeated at least five times.

Reagents—Conductance (G_j) measurements were made at room temperature (22–24 °C) after replacing the culture medium with Tyrode's solution containing 144 mM NaCl, 5.4 mM KCl, 1 mM $MgCl_2$, 2.5 mM $CaCl_2$, 0.3 mM NaH_2PO_4, 5 mM HEPES, and 5.6 mM glucose (buffered to pH 7.4 with NaOH). Low resistance (1.5–2.5-megaohm) patch pipettes were backfilled with a filtered solution containing 140 mM KCl, 0–5 mM MgATP, 5 mM EGTA, 10–14 mM glucose, 0.1 mM GTP, and 10 mM HEPES (buffered to pH 7.2 with KOH).

C3 and Ia-C3 were obtained as described previously (16). CNF-1 was a generous gift of Prof. Patrice Boquet (INSERM U452, Faculté de Médecine, Nice, France). Y-27632 ((*R*)-(+)-*trans*-*N*-(4-pyridyl)-4-(1-aminoethyl)-cyclohexanecarboxamide, 2HCl), the most widely used inhibitor of Rho-associated coiled coil-containing kinase (ROCK), can also inhibit two other Rho effector kinases (see 21), citron kinase (CRIK) and protein kinase novel (PKN) *in vitro* although with K_i values 20 times higher (22), was purchased from Calbiochem. All other chemicals, unless otherwise stated, were obtained from Sigma, including phalloidin, cytochalasin D, and the adenosine analogue 5,6-dichloro-1-β-D-ribofuranosylbenzimidazole.

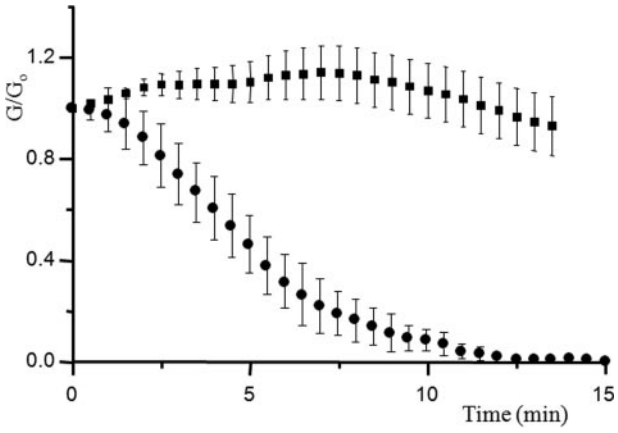

FIGURE 1. **In whole cell conditions, GTP allowed preservation of cell-to-cell communication between cardiac myocytes.** Both cells were clamped at −70 mV, and one cell was stepped to −80 mV every 30 s, whereas the second cell was maintained at the holding potential. Because of the transjunctional voltage difference, a current crossed the cell-to-cell junction that was compensated by an opposite current supplied by the feedback amplifier connected to the cell maintained at −70 mV. In the absence of ATP (●; $n = 9$), a progressive G_j fading was observed, whereas G_j remained relatively stable when GTP (5 mM) was present (■; $n = 9$); error bars, S.E.M.

Statistical Data—The relative permeability constants, junctional conductances, and junctional plaque sizes are expressed as means ± S.E.

RESULTS

GTP Maintains Cell-to-cell Communication between Rat Ventricular Myocytes—The G_j measured in whole cell conditions between neonatal rat cardiomyocytes was well maintained when experiments were carried out with ATP present in the patch pipette solution at a concentration ≥2 mM (Ref. 4; see also Fig. 6*b*), whereas it rapidly decreased (channel "rundown") to complete closure of the channels within 12–20 min when ATP was absent. This loss of channel activity observed in cardiac myocytes when the activity of PKs is impeded (*e.g.* in ATP-deprived conditions) was interpreted as being due to the unbalanced activity of endogenous protein phosphatase(s) (3) ascribed to the activity of PP1 (4). When ATP was replaced by GTP (5 mM) in the pipette filling solution, G_j also remained relatively stable with time, whereas it rapidly declined when ATP was absent (Fig. 1) or replaced by another nucleotide, *e.g.* its poorly hydrolyzable analog AMP-PNP (3).

The first hypothesis to explain this ability of GTP to preserve GJIC would be that GTP can serve as co-substrate to the up to now unidentified PK that would counterbalance PP1 activity. Casein kinase-II phosphorylates different substrates in the presence of either ATP or GTP (23); this enzyme was detected in highly purified plasma membrane preparations from rat (*e.g.* liver (24)) and was found to be able to phosphorylate a connexin (Cx45.6, an avian counterpart of rodent Cx50) *in vitro* (25). However, this hypothesis had to be discarded because casein kinase-II inhibition by the adenosine analogue 5,6-dichloro-1-β-D-ribofuranosylbenzimidazole (26) had no effect on the cell-to-cell diffusion of a fluorescent dye quantified by means of the FRAP technique. The mean rate constants of dye diffusion, *k*, measured in the same cell pairs before and after 5,6-dichloro-1-β-D-ribofuranosylbenzimidazole exposure were 0.272 ±

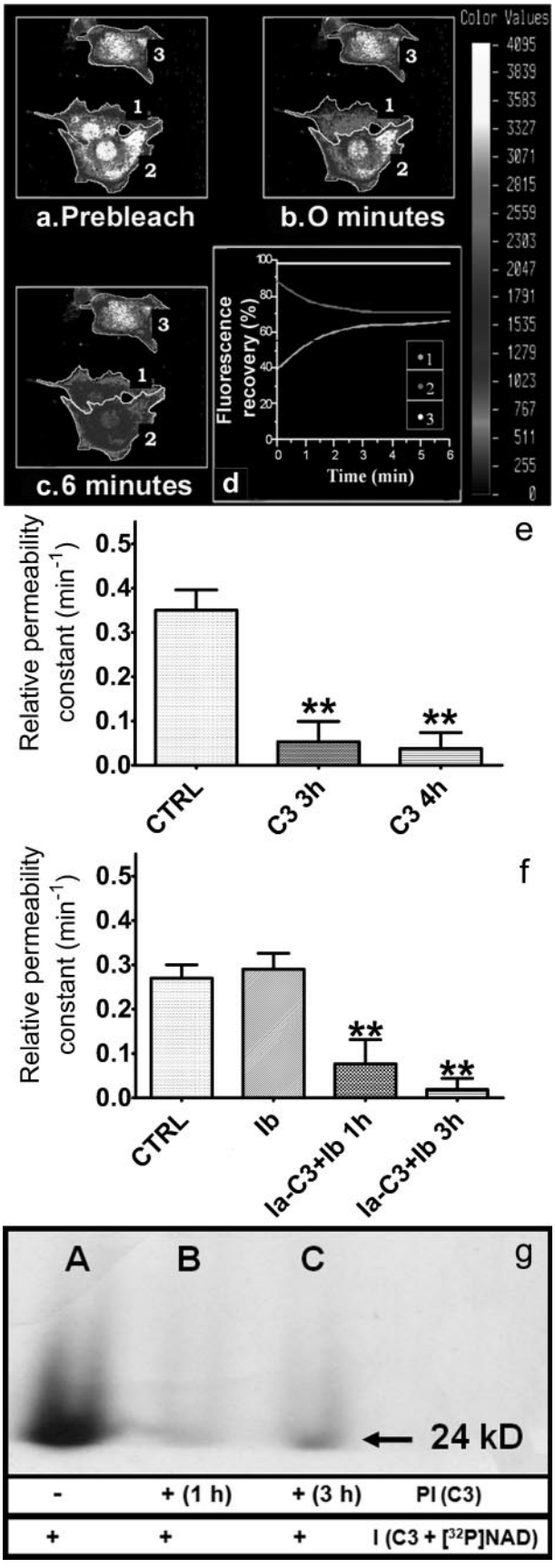

FIGURE 2. **The basal degree of cell-to-cell communication between cardiac myocytes closely depends on RhoA GTPase activity.** *a–c*, the gray density images of fluorescence intensities were obtained by scanning a group of cells in a field with low intensity pulses of laser light. After a prebleach scan (*a*), 6-carboxyfluorescein was photobleached in a selected area (*cell 1*) by means of strong illumination, and the light emission was recorded just after the bleaching (*b*) and 6 min later (*c*) in the bleached cell (*1*), in the neighbor cell (*2*), and in an isolated cell (*3*). The evolution of the fluorescence levels in the selected cells was compared in the same set of cells in control conditions and then after drug exposure. *d*, typical example of the time course of the fluorescent emission in bleached cells in control conditions, represented in percentage of the prebleach emission *versus* the time after photobleaching. *e*, incubation with the exoenzyme C3 for 3 h (*middle column*) or 4 h (*right column*) compared with control (*left column*) markedly reduced the relative permeability constants (*k*) of the fluorescence recovery. $n = 36$, 36, and 33 for *first*, *second*, and *third columns*, respectively. *f*, the active chimeric transport system Ia-C3 (5 μg/ml) + Ib (8 μg/ml) also reduced (*third* and *fourth columns*) the cell-to-cell dye diffusion, whereas the inactive form (*Ib*) had no effect (*second versus first column*). For the *first* to *fourth columns*, $n =$ 22, 22, 19, and 22, respectively. *g*, cardiac myocytes were preincubated (*PI*) without (*A*) or with (*B* and *C*) C3 (25 μg/ml) for 1 (*B*) or 3 h (*C*). The cells were washed and homogenized, and the homogenate was submitted (*I*) to ADP-ribosylation at 37 °C for 1 h in a medium containing 2.5 mM $MgCl_2$, 1 mM ATP, 2 μM [^{32}P]NAD (1000 Ci/mmol), and 25 μg/ml C3. The proteins were separated using 12% PAGE-SDS, the gel was autoradiographed, and the radiolabeled C3 substrate was visualized as a 24-kDa protein. The experiment shown is representative of two separate experiments. *CTRL*, control; **, $p < 0.001$, *error bars*: S.E.

0.011 and 0.270 ± 0.014 min^{-1} ($n = 11$), respectively. The ability of GTP to prevent other channel rundowns in whole cell patch clamp conditions frequently suggests a contribution of small GTPase proteins in maintaining basal channel activities so the possible involvement of RhoA in the control of the strength of intercellular coupling in cardiac myocytes was examined.

Involvement of the Small GTPase Rho in the Modulation of GJIC between Cardiac Myocytes—The main junctional protein present in cardiac myocytes, Cx43, can associate with different proteins (for a review, see Ref. 27), including ZO-1 (8, 9), which functions as a scaffolding protein linking the transmembrane junctional proteins to the actin cytoskeleton (and signal transduction molecules). Moreover the β-actin-binding protein drebrin can interact with the COOH-terminal domain of Cx43 (28), adding a second possibility for actin filament/Cx43 interactions.

The Rho family of small GTPases is known as a major regulator of cellular junctions and of actin cytoskeleton (29). Moreover RhoA is involved in the maintenance of cardiac myocyte morphology (30). C3 is an ADP-ribosyltransferase from *Clostridium botulinum* that irreversibly inactivates RhoA by covalent modification. This exoenzyme ADP-ribosylates mostly RhoA (and to a lesser extent RhoB and RhoC), causing inhibition of RhoA-induced functions, such as the formation of stress fibers, focal adhesion, or the regulation of cell motility. C3 is not taken up into all cells because it lacks cell-binding and translocation domains. *Clostridium perfringens* iota toxin consists of two unlinked proteins: Ia, the enzymatic component that ADP-ribosylates G-actin, and Ib, the binding component that is required for internalization into cells. A chimeric toxin, Ia-C3 (presenting only a C3 enzyme activity), was constructed to permit a ubiquitous entry of C3 into cells using Ib (16).

The effects of these toxins on the cell-to-cell diffusion of a fluorescent dye was investigated in ventricular myocytes by means of the FRAP technique as illustrated in Fig. 2. After the cells were loaded with 6-carboxyfluorescein, the computer-generated images of the fluorescent dye distribution were

obtained before (Fig. 2*a*) and then respectively just after photobleaching (Fig. 2*b*) and 6 min later (Fig. 2*c*) in Tyrode's solution before or after exposure of the cells to active agents. The unequal fluorescence levels inside one cell and between different cells reflect variations in cell thickness. In the first approximation, in interconnected cells, the redistribution of 6-carboxyfluorescein after photobleaching takes place in a system of two compartments, namely the photobleached cell and the set of unbleached adjacent cells, separated by gap junctional membranes acting as a diffusion barrier. The graphs showing typical examples of the evolution with time of the integrated fluorescence intensities after photobleaching are illustrated Fig. 2*d*. Immediately after the photobleaching of the selected cell, its light emission was reduced to about 40% of its initial level, and then a rise in fluorescence emission took place with a monoexponential time course with a concomitant decrease in the adjacent cell. The rate constant k provides an estimation of the relative permeability of the gap junction of the tested cell pair. In control experiments, no significant change in k was noticed when up to four consecutive photobleachings were performed on the same cells (31).

C3 significantly reduced k when compared in cardiac myocytes before and after incubation with C3 (25 μg/ml) for 3 h in culture medium. k was indeed lowered from 0.35 $\pm$ 0.046 min^{-1} in control conditions to 0.053 $\pm$ 0.046 min^{-1} after incubation with C3 (25 μg/ml) for 3 h ($n = 36$; Fig. 2*e*). The kinetics of cell-to-cell dye diffusion continued to decrease with longer exposures with k lowered to 0.038 $\pm$ 0.036 min^{-1} ($n = 33$) after 4 h. The active chimeric transport system for C3 (Ia-C3, 5 μg/ml; Ib, 8 μg/ml), used as control, similarly reduced the junctional coupling (k was reduced from 0.27 $\pm$ 0.03 ($n = 22$) to 0.076 $\pm$ 0.054 ($n = 19$) and 0.019 $\pm$ 0.025 min^{-1} ($n = 22$)) after 1 and 3 h, respectively, whereas Ib had no effect (k = 0.29 $\pm$ 0.036 min^{-1}; $n = 22$; Fig. 2*f*).

To ensure that RhoA was ADP-ribosylated in cellula by C3, ventricular myocytes were pretreated with C3 for 1 or 3 h. Then cells were harvested, and the homogenates were reincubated with [^{32}P]NAD and C3 at 37 °C for 1 h. Autoradiography of SDS-PAGE-migrated homogenates revealed that RhoA in untreated samples presented a classical ADP-ribosylation, whereas in C3-pretreated samples (for both 1 and 3 h), no further ADP-ribosylation occurred, showing that RhoA was already ADP-ribosylated during the preincubation (Fig. 2*g*).

Further evidence for a role for Rho in regulation of cardiac GJIC was obtained using CNF-1, an exotoxin of *Escherichia coli* that constitutively activates the small GTPases, including Rho (as well as Rac and Cdc42) by the deamidation of Glu-63 of p21 Rho. Cells exposed to CNF (200 ng/ml) exhibited a significant increase of the kinetics of cell-to-cell dye transfer (Fig. 3); k was increased from 0.31 $\pm$ 0.015 ($n = 41$) in control conditions to 0.44 $\pm$ 0.033 ($n = 10$), 0.46 $\pm$ 0.026 ($n = 17$), and 0.47 $\pm$ 0.020 min^{-1} ($n = 18$) after 1, 3, and 6 h, respectively ($p < 0.01$ by Student's paired t test).

RhoA Activity Affects GJIC without Major Cellular Redistribution of Junctional Plaques or Changes in the Cx43 Phosphorylation Pattern—The immunocytochemical localization of Cx43 proteins examined by confocal microscopy on cardiomyocytes in control conditions showed, as reported previously

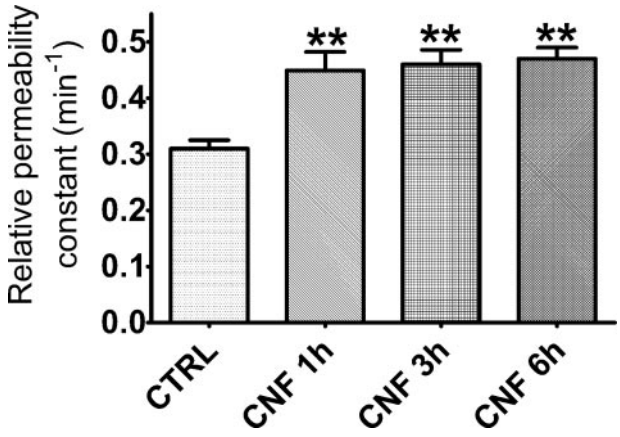

FIGURE 3. **The strength of intercellular coupling between cardiac myocytes was enhanced when RhoA GTPase activity was stimulated.** Incubation of cells with the exotoxin CNF-1 (200 ng/ml) for 1, 3, or 6 h significantly enhanced the kinetics of intercellular dye diffusion. For *first* to *fourth columns*, $n = 41$, 10, 17, and 18, respectively. *CTRL*, control, **, $p < 0.001$, *error bars*, S.E.

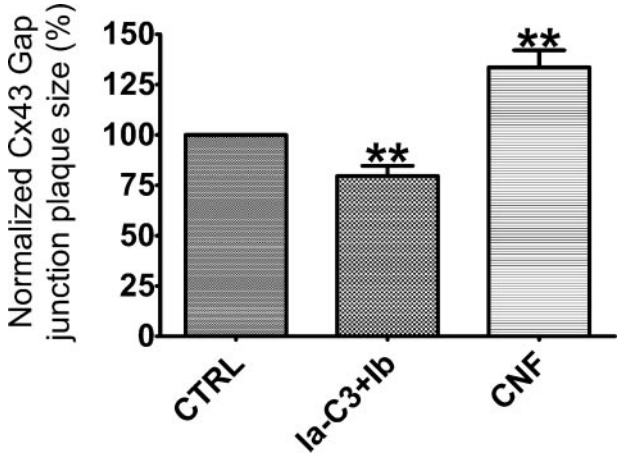

FIGURE 4. **The size of Cx43 junctional plaques was influenced by RhoA activity.** The mean size of Cx43 plaques observed in optical sections was significantly reduced (0.49 $\pm$ 0.025 μm^2, $n = 14$; *middle column*) in C3-treated cells and increased (0.83 $\pm$ 0.038 μm^2, $n = 13$; *right column*) in CNF-exposed cells compared with control cardiomyocytes (0.62 $\pm$ 0.022 μm^2, $n = 41$; *left column*). *CTRL*, control, **, $p < 0.001$, *error bars*, S.E.

(see for example Ref. 32), a prevalence of the phosphorylated form of Cx43 characterized by a punctate immunopositive reaction for total Cx43 predominantly observed at the plasma membrane, typical of Cx43 junctional aggregates, whereas the light labeling of the unphosphorylated Cx43 was observed at the cell-cell interface but also at the perinuclear border (data not illustrated). Cx43 labeling appeared to be moderately reduced after C3 exposure and increased after treatment with CNF (see Figs. 7 and 10). After C3 exposure, the mean size of individual Cx43 plaques observed in optical sections was significantly reduced (Fig. 4) but, however, to a lesser extent than the intercellular coupling (the respective reductions were -20.67 ± 5 *versus* $-91.42 \pm 9.52\%$). When cells were exposed to CNF, the mean size of the junctional plaques was substantially increased ($+32.48 \pm 8.44\%$) although less than the level of cell-to-cell coupling in these conditions ($+48.58 \pm 8.52\%$). Immunoblot analysis performed on rat ventricular myocytes in control conditions or treated with C3 or CNF for 3 h or even 6 h did not reveal noticeable difference in the ratios between the

electrophoretic bands of the protein (Fig. 5), suggesting that the serine phosphorylation of Cx43 was not altered by C3 or CNF exposure by either inhibition or activation of RhoA activity.

The Integrity of the Actin Microfilament Network Is Essential to Preserve Cell-to-cell Communication between Cardiac Myocytes—Members of the Rho family of small GTPases frequently act as molecular switches regulating the organization of the cortical cytoskeleton, and actin cytoskeleton rearrangements are the basis of many fundamental processes of cell biology. So the possible involvement of the actin cytoskeleton in the modulation of the gap junctional permeability was investigated using two actin-binding proteins known to alter actin polymerization, phalloidin and cytochalasin D.

Phalloidin, an alkaloid compound produced by the mushroom *Amanita phalloides*, binds to actin filaments, preventing their depolymerization by shifting the equilibrium from monomers toward filaments (for a review, see for example Ref. 33).

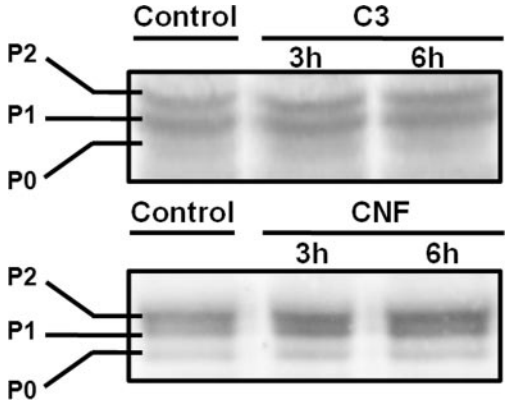

FIGURE 5. **Activation or inhibition of RhoA affects GJIC without concomitant change in the ratios of the Cx43 phosphoisoforms.** *Top*, rat cardiomyocytes in control conditions or after exposure to C3 for 3 or 6 h. 20 μg of each sample were loaded on a polyacrylamide gel and subjected to SDS-PAGE, and the protein was transferred onto nitrocellulose membrane. *Bottom*, rat cardiomyocytes in control conditions or after exposure to CNF for 3 or 6 h. 20 μg of each sample were loaded on a polyacrylamide gel and subjected to SDS-PAGE, and the protein was transferred onto nitrocellulose membrane. The presence of Cx43 was revealed by means of an anti-Cx43 antibody; the *arrows* on the *left* indicate the position of the nonphosphorylated form (*P0*) and phosphorylated forms (*P1* and *P2*). Shown are representative blots of five separate experiments in each case.

Cytochalasin D is an alkaloid drug produced by the mold *Helminthosporium* sp. that prevents actin polymerization, caps the barbed end of actin filaments, and binds to monomeric actin *in vitro*. All these effects lead to a fall in the rigidity of actin gels and to a decrease in the actin filament length.

Pairs of cardiomyocytes were preincubated with phalloidin (10 μM for 4 h), and then G_j was measured in whole cell conditions. When the experiments were carried out with a patch pipette solution devoid of ATP, G_j gradually declined until there was complete interruption of the cell-to-cell communication within about 12 min with a time course very similar to the one recorded in the absence of phalloidin (Fig. 6*a*). In contrast, when the phalloidin concentration in the preincubation bath was increased to 20 μM, the kinetics of channel rundown was slowed down, and this effect was still more pronounced when the alkaloid concentration was increased to 30 μM. Stabilizing the cytoskeleton by exposure to phalloidin delayed the interruption of cell-to-cell communication observed in ATP-deprived conditions.

In an attempt to distinguish whether, besides an altered cell surface expression of junctional channels, the disruption of the cytoskeletal actin network might affect the level of cell-to-cell coupling, the acute effects of cytochalasin D added (10 μM) to the patch pipette solution were examined. Cytochalasin D very rapidly and markedly reduced the strength of cell-to-cell coupling despite the presence of ATP (5 mM; Fig. 6*b*). Hence the level of junctional intercellular communication appears to depend on the actin filament dynamics.

Anti-actin staining of cultured cardiomyocytes in control conditions revealed (Fig. 7, *lower row*) that actin was predominantly organized into striated fibers (myofibrils), whereas a minor part was observed as non-striated actin fibers previously suggested to represent premature forms of myofibrils (premyofibrils; Ref. 34). After exposure to C3 (25 μg/ml for 3 h), no obvious change was observed in the actin labeling (Fig. 7) as reported previously. Into the same cell type, microinjection or transfection of C3 transferase did not disrupt actin muscle fiber morphology (35), and prolonged exposure (48 h) to a high concentration (up to 200 μg/ml) of exoenzyme C3 from *C. botulinum* or recombinant C3 only partially affected the pattern of actin staining (7).

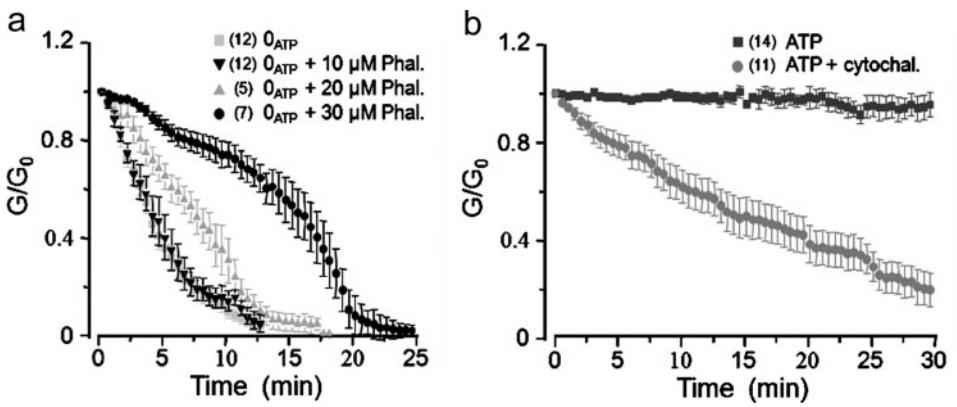

FIGURE 6. **The degree of cell-to-cell communication between cardiac myocytes depends on the integrity of the actin microfilament network.** *Left*, preincubation of the cells for 4 h with phalloidin (*Phal.*) at concentrations $\geq$ 20 μM, delayed the channel rundown in ATP-deprived conditions. *Right*, the presence of cytochalasin D (*cytochal.*; 10 μM) in the pipette filling solution markedly reduced the junctional coupling despite the presence of ATP (5 mM). In each case, *n* is indicated in *parentheses*, *error bars*, S.E.

C3 and CNF Do Not Influence GJIC through Modifications of Adhesive Interactions between Cardiac Myocytes—The formation and preservation of gap junctions between cardiac myocytes depend on the proper cytoarchitecture of the cardiomyocytes. The cell adhesion molecule N-cadherin mediates strong homophilic cell-cell adhesion via linkage to the actin cytoskeleton; N-cadherin appears before Cx43 at newly established cell-cell contact sites between the myocytes (36). Because in some cell types Rho signaling plays important roles in the formation and/or main-

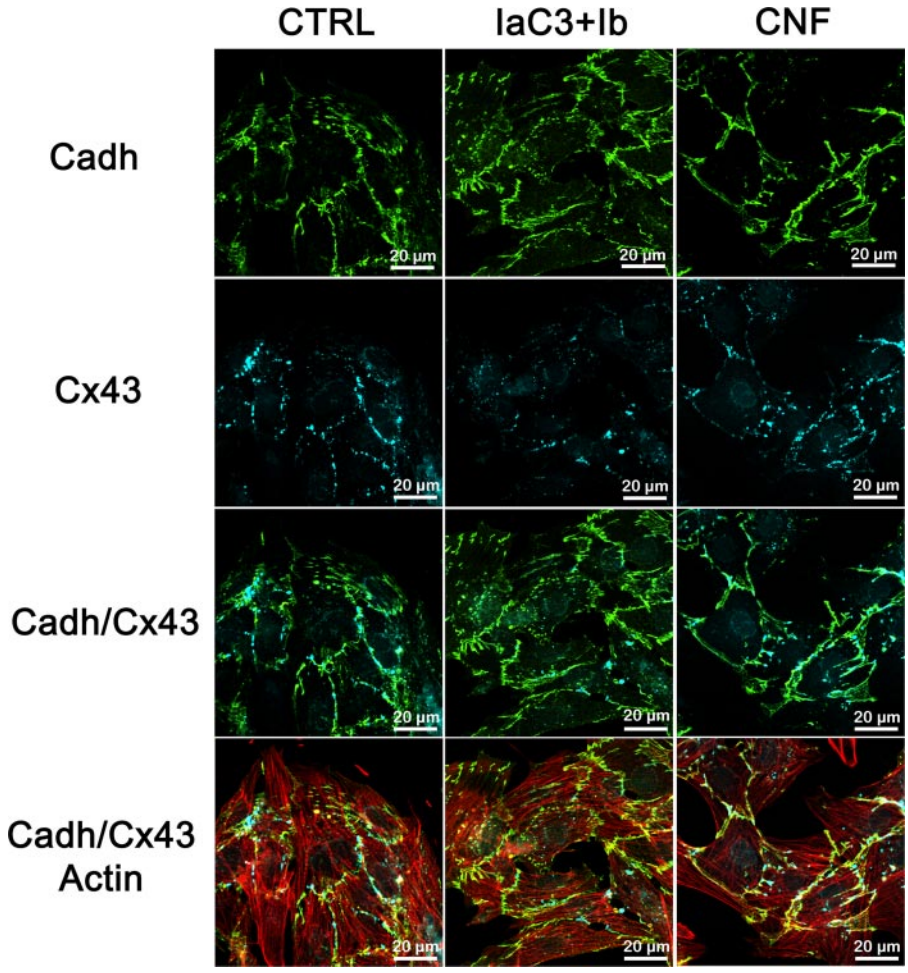

FIGURE 7. **N-Cadherin immunolocalization was not noticeably modified after RhoA inhibition or activation.** Representative sets of confocal optical sections showing N-cadherin (*Cadh*) (green, *top row*), Cx43 (blue, *second row*), merged (*third row*) distributions before (*left column*) and after exposure of the cells to C3 (*middle column*) or CNF (*right column*); in addition, actin (*red*) was also labeled (*bottom row*). Similar results were obtained from 3 separate experiments. *CTRL*, control.

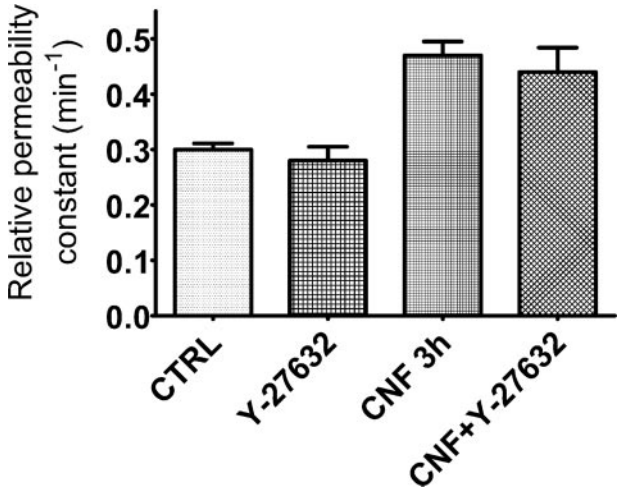

FIGURE 8. **The Rho-kinase inhibitor Y-27632 neither alters the basal degree of junctional coupling between cardiac myocytes nor prevents its enhancement by CNF.** Exposure of the cells for 1 h to Y-27632 (10 μM) had no noticeable effect on relative permeability constants (*k*) (*second versus first column*); preincubation of the cells for 1 h with 10 μM Y-27632 did not prevent the *k* enhancement observed after exposure of the cells to CNF for 3 h (*fourth versus third column*). For *first* to *fourth columns*, $n = 46$, 17, 17, and 11, respectively. *CTRL*, control, *error bars*, S.E.

tenance of cadherin-dependent adhesion, the possible involvement of N-cadherin in the effects on GJIC of RhoA activation or inhibition was examined. As illustrated in Fig. 7 (*upper row*), neither inhibition of RhoA by C3 nor its activation by CNF noticeably affected immunolocalization of N-cadherin in ventricular myocytes.

Rho Does Not Affect GJIC via Rho Downstream Kinase Effectors (ROCK, CRIK, and PKN)—Many of the Rho effects on the actin cytoskeleton are considered to result from the activation of its downstream protein kinase effectors, particularly ROCK. To assess their potential contribution in RhoA-mediated effects on GJIC, the dye coupling kinetics were compared before and after the cardiomyocytes were infused for 1 h with a culture medium containing the ROCK inhibitor Y-27632 (37). If K_i values of Y-27632 are about 20 times higher for CRIK and PKN than for ROCK (see Ref. 22), then Y-27632 used in the present experimental conditions at 10 μM concentration is expected to also significantly inhibit their activity without altering the activities of other protein kinases (*e.g.* PKA or PKC; Ref. 38). The lack of effect of Y-27632 on the cell-to-cell dye diffusion in basal conditions ($k = 0.28 \pm 0.025$ min^{-1} ($n = 17$) after 1 h *versus* 0.30 ± 0.011 min^{-1} ($n = 46$) in control conditions) or even after prolonged exposures (3 h; $n = 27$; data not illustrated) as well as its inability to prevent the increase in the strength of cell-to-cell communication caused by CNF ($k = 0.44 \pm 0.044$ min^{-1} ($n = 11$) in cells preincubated with Y-27632 compared with 0.47 ± 0.025 min^{-1} ($n = 18$) in its absence), see Fig. 8, shows that the tonic effects of Rho on the permeability of junctional channels are not mediated through the activity of the most common downstream kinase effectors (particularly ROCK, CRIK, or PKN) without, however, excluding potentially Y-27632-insensitive PKs (*e.g.* a threonine kinase) or lipid kinases (*e.g.* phosphatidylinositol-4-phosphate 5-kinase).

RhoA Influences the Strength of Cell-to-cell Communication via the Actin Cytoskeleton—To show evidence of the involvement of the cortical actin cytoskeleton in the modulating effects of RhoA activity on the degree of cell-to-cell coupling, the effects of C3 and of CNF were investigated in cells whose actin cytoskeleton had been stabilized by a prolonged exposure to phalloidin. This treatment significantly increased *k* from 0.31 ± 0.011 min^{-1} ($n = 41$) in control conditions to 0.46 ± 0.015 min^{-1} ($n = 14$; see Fig. 9) after a 4-h exposure to phalloidin.

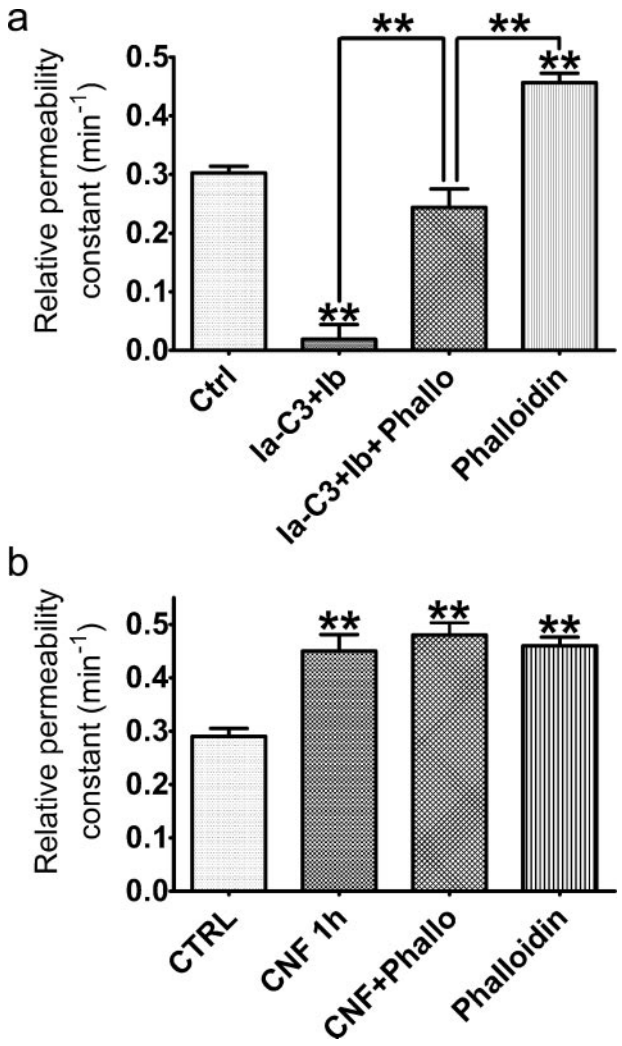

FIGURE 9. **C3 and CNF had limited effects on GJIC between phalloidin-treated cardiomyocytes.** *a*, GJIC was markedly increased in cells treated with phalloidin (*Phallo*, 30 μM) for 4 h; subsequent exposure to C3 reduced GJIC but much less than in the absence of phalloidin. For *first* to *fourth columns*, $n = 41$, 13, 15, and 14, respectively. *b*, in phalloidin-treated cells, CNF treatment for 1 h had no additive effects. For *first* to *fourth columns*, $n = 41$, 10, 14, and 14, respectively. *CTRL*, control, **, $p < 0.001$, *error bars*, S.E.

When the cells were subsequently exposed to modulators of the activity of Rho GTPase, Ia-C3 or CNF, these agents had only very modest effects on the strength of communication (Fig. 9). Ia-C3 exposure indeed reduced the relative permeability constant k to 0.24 ± 0.031 min^{-1} ($n = 15$) compared with 0.017 ± 0.029 min^{-1} ($n = 13$) measured in cells not pretreated with phalloidin, whereas CNF slightly increased k from 0.45 ± 0.031 ($n = 10$) to 0.48 ± 0.023 min^{-1} ($n = 14$).

The fact that the stabilization of the actin cytoskeleton with phalloidin markedly impaired the very important reduction of dye coupling caused by Ia-C3 and that RhoA activation by CNF had no significant additive effects suggests that RhoA influences GJIC via the actin cytoskeleton. Rho GTPases are molecular switches that control a wide variety of signal transduction pathways in all eukaryotic cells. They are known principally for their pivotal role in regulating the actin cytoskeleton. However, up to now, neither actin nor RhoA seemed to directly interact with Cx43 (see Ref. 27), and no sign of Cx43/RhoA co-localization was observed in ventricular myocytes whatever the conditions (in control conditions or after C3 or CNF treatment; data not illustrated). ZO-1, which plays a critical role in the life cycle of gap junctions, is known to cross-link membrane macromolecular complexes to the actin cytoskeleton (39).

RhoA Activity Influences the Cx43/ZO-1 Interaction—Alterations in the Cx43/ZO-1 interactions were observed for example after disruption of intercellular contact between myocytes by partial or complete enzymatic dissociation of myocytes from intact ventricle (13). To examine the possibility of intracellular redistribution of ZO-1 and Cx43 in cells exposed to C3 or CNF, the molecular association of Cx43 and ZO-1 was first investigated by indirect co-immunolocalization experiments. Cx43 and ZO-1 were present at the plasma membrane in cells cultured in the absence (Fig. 10*a*, *left column*) or in the presence of C3 (Fig. 10*a*, *middle column*) or CNF (Fig. 10*a*, *right column*) for 3 h.

The most prominent co-localization of Cx43 and ZO-1 was, as recently reported (11, 12, 40), observed at the junctional plaque perimeter (Fig 10*a*, *bottom row*). Both Cx43 (*top row*) and ZO-1 (*second row*) labelings at the cell periphery appeared modestly reduced after C3 exposure and increased after treatment with CNF (Fig. 10*a*; see also Figs. 4 and 7). The mean size of individual Cx43 plaques observed in optical sections was significantly reduced after C3 exposure and increased after CNF treatment (see Fig. 4) but in both cases to a much lesser extent than the intercellular coupling.

The observation that Cx43/ZO-1 co-localization was increased after C3 exposure and decreased after CNF treatment (Fig. 10*a*) was corroborated by co-immunoprecipitation assays (Fig. 10*b*) where Cx43 was immunoprecipitated from cell lysates and ZO-1-containing complexes were analyzed by Western blotting with anti-ZO-1 antibody; one band around 220 kDa was detected. This band was noticeably increased in C3 conditions and markedly decreased in CNF, reflecting an increase of Cx43/ZO-1 interaction in C3-treated cells and a decreased interaction in CNF-exposed cardiomyocytes.

DISCUSSION

The present study showed that, in rat cardiac myocytes, the RhoA signaling pathway dynamically modulates the permeability of Cx43-made channels. The activation of the RhoA GTPase cascade markedly enhanced the cell-to-cell diffusion of a fluorescent dye, whereas opposite effects were observed after specific inhibition of Rho GTPase-induced functions by ADP-ribosylation of RhoA. Because (i) actin filament depolymerization by cytochalasin D elicited a junctional current rundown despite the presence of ATP whereas (ii) actin filament stabilization by phalloidin slowed down the loss of junctional channel activity in ATP-deprived conditions and markedly reduced the effects of RhoA activation or inactivation, RhoA is likely to control the degree of intercellular coupling via its pivotal role in regulating the actin cytoskeleton.

G-protein signaling cascades have emerged as one of the primary cellular mechanisms for controlling membrane channels; they were found to modulate the activity of different membrane channels, including several Na^+, Ca^{2+}, and K^+ channels (Ref. 41 and references therein), either directly or indirectly. About

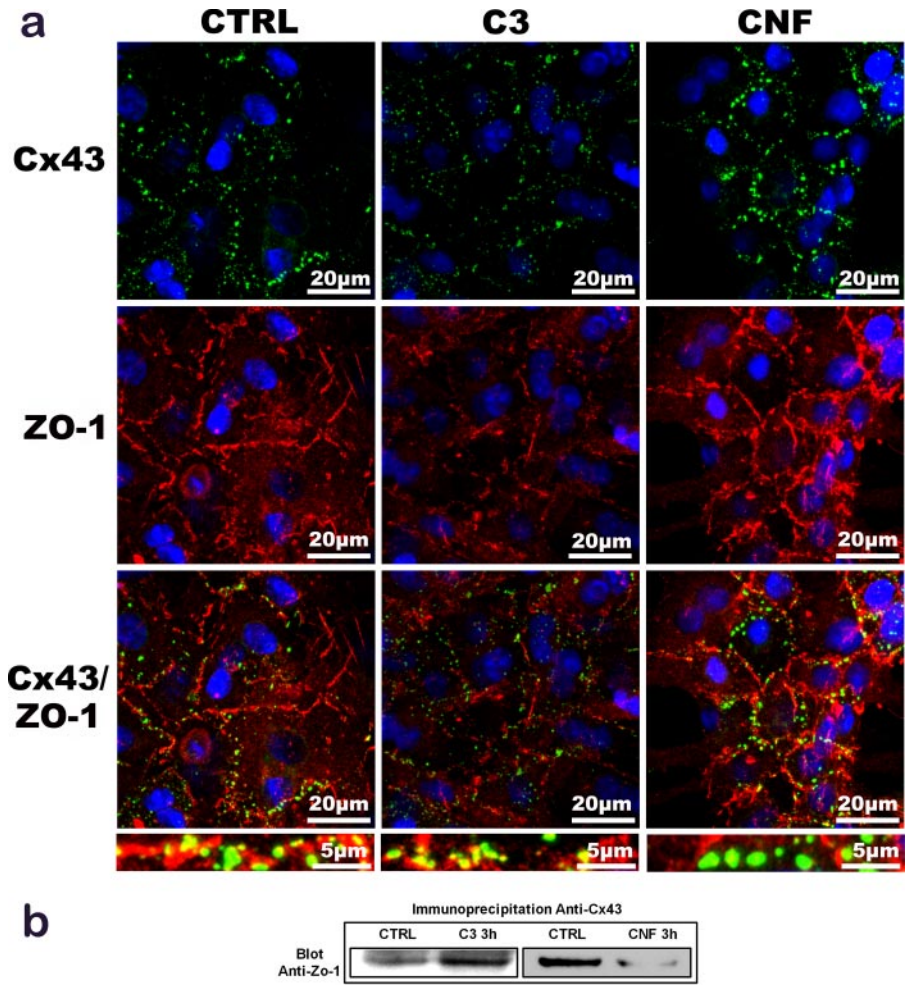

FIGURE 10. **Rho inhibition enhanced the Cx43/ZO-I interaction.** *a*, representative sets of confocal optical sections showing nucleus (*blue*), ZO-1 (*red*), and Cx43 (*green*) distributions before (*left column*) and after exposure of the cells to C3 (*middle column*) or CNF (*right column*). The *lowest row* of images are enlargements of plasma membrane regions. In control cells, both proteins are located at the plasma membrane. *b*, cardiomyocyte lysates were immunoprecipitated with anti-Cx43 antibodies. Immunoprecipitates were analyzed by ECL Western blotting immunodetection with anti ZO-1 antibodies. It has to be noted that the blots were done independently with different exposure times. Indeed in the *left panel*, because a large amount of ZO-1 was co-immunoprecipitated with Cx43 after C3 treatment, the chemiluminescence reaction had to be stopped when this sample began to saturate. In contrast, in the *right panel*, it was necessary to saturate the control sample to allow visualization of the ZO-1 band revealed by chemiluminescence in the CNF-treated sample that was virtually invisible with normal exposures. ZO-1 was detected at the predicted size of 220 kDa. Shown are representative blots of five separate experiments in each case. *CTRL*, control.

30 potential effector proteins, including different subsets of PKs, have been identified that interact with members of the Rho family, but a significant number of mammalian Rho GTPases are still poorly characterized (for reviews, see Refs. 21 and 42). Previous studies on the possible involvement of G-proteins in the modulation of GJIC focused on the larger, heterotrimeric GTPases (activated by seven transmembrane receptors for hormones and neurotransmitters at the cell surface) and showed they influence Cx43 trafficking because their inhibition by the pertussis toxin inhibited GJ assembly in a degree comparable to that of the trafficking inhibitors brefeldin A or monensin (43). Only a few studies have reported influence of the smaller, monomeric, Ras-related G-proteins. Postma *et al.* (44) showed that Cx43-based junctional communication was rapidly but transiently disrupted upon activation of various G-protein-coupled receptors, including those for lysophosphatidic acid, thrombin, and neuropeptides, through a signaling pathway involving c-Src. In mouse striatal astrocytes, sphingosine 1-phosphate caused an inhibition of GJIC through an activation of both G_i and Rho GTPases (45). In rabbit corneal epithelial cells, C3 significantly reduced within 6 h the Cx43 gap junction assembly (46), whereas in embryonic stem cell-derived cardiomyocytes, a 3-h treatment resulted in a significant up-regulation of Cx40, Cx43, and Cx45 transcript levels, whereas 6- or 16-h exposures had no effects on connexin transcript levels (47). The data of the present study show that, in rat ventricular myocytes, GJIC strength closely depends on RhoA GTPase activity because activation or inhibition of RhoA activity each result in parallel up- or down-regulations of GJIC; in contrast, the inhibition of the most common RhoA downstream kinase effectors by Y-27632 had no effect. In mouse ventricular myocytes, the inhibition of RhoA (but not Rac1 or Cdc42) decreased the density of L-type calcium currents, whereas Y-27632 had no effect (48).

In rat ventricular myocytes, all treatments able to shift the protein phosphorylation/dephosphorylation balance toward dephosphorylation led to disruption of the junctional communication, an effect mainly ascribed to PP1 activities (see 49). Myocardial ROCK was suggested to decrease the activity of PP1δ (also known as myosin phosphatase) through phosphorylation of its regulatory subunit (myosin-binding phosphatase targeting; Ref. 50). The lack of influence of Y-27632, consistent with the absence of effect of staurosporine (a serine/threonine PK inhibitor considered to be more potent than Y-27632 in inhibiting ROCK) on the cell-to-cell coupling (51), indicates that RhoA does not influence the junctional permeability via a depressing action on PP1 activity through its downstream effector ROCK. In mouse striatal astrocytes, Rouach *et al.* (45) also recently reported that neither Y-27632 (30 μM) nor staurosporine (1 μM) used alone had effects on cell-to-cell dye coupling.

The Rho subfamily of Ras-related GTP-binding proteins are well known to act as molecular switches regulating the organization of the actin cytoskeleton. The constitutive activation of Rho proteins by CNF-1 for example induced a polarized reorganization of F-actin even in the presence of Y-27632 (52). The

modulation of actin dynamics involves a complex interplay of the Ras G-proteins where Rac and Rho frequently have antagonist effects, particularly for cell motility. C3 inactivates Rho proteins, but CNF-1 activates both Rho and Rac by deamidation of glutamine 61/63, amino acids essential for GTPase activity. But CNF-1-activated Rac vanished in CNF-1-treated cells due to proteolytic degradation, whereas the amount of RhoA was only slightly influenced (see Ref. 53). The observed sustained GJIC enhancement (still more pronounced after 6 h of CNF exposure) then appears to result from Rho activation. Moreover alterations in membrane junctions ascribed to enhanced Rac activity usually do not affect ZO-1 immunolocalization, whereas effects attributed to Rho activation are accompanied by ZO-1 displacement. For example, this was the case in T84 intestinal epithelial cells where CNF-1 on the one hand caused both a profound reduction in tight junction gate function and a dramatic redistribution of ZO-1 compatible with enhanced RhoA activity, and on the other hand, subtle alterations in adherens junction protein localization, were ascribed to Rac over Rho activity (52).

F-actin disrupters (*e.g.* cytochalasin B) induced a rapid assembly of gap junctions in prostate epithelial cells *in vitro* (54), whereas they prevented forskolin-induced Cx43 clustering at cell-cell contacts between rat Morris hepatoma cells (55). Conversely in cultured astrocytes of embryonic rat, gap junction inhibitors, which do not prevent the formation but rather the function of gap junctions, caused both a discordance of actin stress fibers between neighboring cells and a reduction of calcium wave propagation (56). Taken together, these studies suggested the existence of cooperative mechanisms involved in the interactions between F-actin and Cx43 channels.

The decline in channel activity in ATP deprived conditions is also a hallmark of several other membrane channels, including several inwardly rectifying K^+ channels (IKir), observed in both excised patches (57) and whole cell conditions (58, 59). In the latter configuration, a channel rundown, as for gap junctional channels, was observed when cells were exposed to metabolic inhibitors or dialyzed with ATP concentrations <2 mM or when ATP was replaced by its non-hydrolyzable analogue AMP-PNP. For both gap junctional and inwardly rectifying K^+ currents, the channel activity remained sustained when ATP was replaced by GTP in the pipette solution (59) and when the activity of endogenous phosphatases was inhibited in ATP-deprived conditions (3, 58) and was lowered when the endogenous phosphatase activity was enhanced (4, 58). But the behavior of channels differed when cells were exposed to actin-depolarizing agents: cytochalasin B had no effect on the activity of inwardly rectifying K^+ channels (58), whereas in the present study, cytochalasin D rapidly reduced gap junctional conductance. Similar short term applications (10–15 min) of this agent also modulated the activity of other membrane channels, of Kv4.2 currents for example, where the current density was altered but the activation or inactivation properties of the channels remained unmodified, suggesting an effect on open probability (60).

The stabilization of the actin cytoskeleton by phalloidin significantly increased GJIC; phalloidin also greatly potentiated the activities of some other membrane channels, for example fast Na^+ (INa (61)) or L-type Ca^{2+} (62, 63) channels, an augmentation primarily ascribed by Kim *et al.* (63) to a phalloidin-induced G-actin polymerization. An intact actin cytoskeleton is essential to allow the translocation of Cx43 to the plasma membrane (64), but the acute effects of the actin depolymerization agent show that the actin cytoskeleton also modulates the gating of the junctional channels very likely by lowering their open probability. This result is consistent with the limited changes in Cx43 subcellular localization observed when the intercellular coupling was drastically reduced after C3 exposure, suggesting that RhoA modulates junctional channel function without interfering with membrane trafficking. The actin cytoskeleton dynamics may have an important influence in the modulation of cell-to-cell junctional communication comparable to the central importance it has in determining the localization and functional activity of many other membrane channels (Ref. 60 and references therein). This contrasts with the very limited influence of the microtubular network because if tubulin binds to the carboxyl-terminal tail of Cx43 Giepmans *et al.* (65) showed that intact microtubules were dispensable for the regulation of Cx43 gap junctional communication.

The actin cytoskeleton is not known to directly interact with gap junction proteins (see Ref. 27); zonula occludens proteins, particularly ZO-1, a 220-kDa peripheral membrane protein, are both actin-binding and cross-linking proteins and tether transmembrane proteins (*e.g.* occludin, claudin, junctional adhesion molecule, or gap junction proteins) to the actin cytoskeleton. ZO-1 and Cx43 were found co-localized in different cell types, including cardiac myocytes (9, 66). ZO-1 was proposed to provide a docking site that temporarily secures the different connexins in gap junction plaques at the cell-cell boundary; different domains of ZO-1 serve as docking modules for kinases and phosphatases that interact with the different connexin polypeptides (67). In the present study, C3 caused a reduction in ZO-1 labeling and in the intercellular coupling, whereas CNF had opposite effects. RhoA inhibition caused an increase of the Cx43/ZO-1 association accompanied by a decrease in junctional plaque size, whereas RhoA activation had opposite effects, a reduction of the Cx43/ZO-1 association and an augmentation in junctional plaque size. Such variations are consistent with the observations of Hunter *et al.* (12) and Zhu *et al.* (11) who noticed that, in neonatal cardiomyocytes, a reduction of peripherally associated ZO-1 was accompanied by a significant increase in plaque size.

The clustering of cell surface proteins is routinely assumed to be due to relatively static interactions with scaffolding proteins that in turn are attached to cytoskeletal components. Cytoskeleton-based perimeter fences have recently been reported to selectively corral a membrane protein subpopulation of channels (Kv2.1 channels) to generate stable 1–3-μm^2 clusters (68). These authors noticed that despite the stability of these microdomains the channels retained within the cluster perimeter were surprisingly mobile, showing that the clustering did not result from a static scaffolding-based structure. Connexin channels clustered in gap junctional plaques share these characteristics where ZO-1 is preferentially localized at the periphery of the plaques (11, 12), suggesting that a ZO-1-actin perimeter fence could selectively corral gap junction channels. The

reduction of Cx43/ZO-1 interaction significantly increased the size of Cx43 plaques (12, 69) with, in the latter study, a concomitant reduction in their overall number. The reduction of the plaque size observed in the present study might call attention to the "ZO-1 ring" surrounding Cx43 plaques.

Divergent roles have been proposed for Cx43/ZO-1 interaction, including the control of gap junction formation and localization of gap junction plaques, internalization of Cx43, and its targeting for endocytosis (for review, see 27). According to van Zeijl *et al.* (70), phosphatidylinositol 4,5-bisphosphate might regulate junctional communication in an indirect manner, for example, via a Cx43-associated protein that modifies the Cx43 regulatory tail and thereby the channel functions. In osteoblastic cells, the disruption of the Cx43/ZO-1 interaction with a connexin-binding fusion protein derived from ZO-1 disrupted gap junction formation and function, whereas overexpression of ZO-1 enhanced both junctional plaques and GJIC (71). A dramatic reduction in ZO-1 expression coinciding with reduced Cx43 staining was also observed in the failing human heart (72). The down-regulation of ZO-1 in N/N1003A lens epithelial cells also resulted in loss of dye transfer activity without altering the total amount of Cx43 protein in the cells (40).

Zonula occludens proteins are also present in the other intercellular junctions, tight junctions and adherens junctions, where they link transmembrane proteins with the underlying actin cytoskeleton (for a recent review, see Ref. 73). Both tight junctions and adherens junctions are regulated in part by this affiliation with the F-actin cytoskeleton. C3 and CNF both affected barrier functions of tight junctions and caused ZO-1 redistribution (see Ref. 74). As the existence of stable mechanical contacts based on anchoring junctions is of essential importance for the formation and stabilization of gap junctions, the GJIC dependence on RhoA activity might reflect an indirect effect through an action on adhesion junctions. Rho for example has been shown to negatively regulate cadherins (through the actin cytoskeleton frequently), and evidence also exists that cadherin-mediated cell-cell contact activates Rac1 and/or Cdc42, depending on the experimental system, and decreases RhoA activity (see Ref. 75). In mouse for example, a cardiac-restricted deletion of N-cadherin resulted in disassembly of the cardiac intercalated disc structure and a significant decrease in Cx43 in the working myocardium where the electrical coupling was lost (76, 77). However, if Matsuda *et al.* (78) also observed an inhibition of Cx43 accumulation in cultured cardiac myocytes of newborn rat after functional inhibition of N-cadherin, the inhibition of Rho family proteins by Rho-GDP dissociation inhibitor significantly attenuated the accumulation of Cx43 but not that of N-cadherin, suggesting that, in these cells, the localization of Cx43 was determined through the Rac1 downstream pathway of N-cadherin. Anderson *et al.* (46) reported that E-cadherin adherens junctions are not a prerequisite for the assembly of Cx43 gap junctions in corneal epithelial cells. When CNF-1 was used to activate Rho GTPases, only subtle alterations of adherens junctions were observed (52). In rat ventricular myocytes, neither inhibition of RhoA nor its activation noticeably affected immunolabeled N-cadherin, but conversely Rho family proteins, which are known to be signal transducers downstream of cadherin (75) adherens junctions, might then influence GJIC. N-cadherin for example was found to be able to modulate voltage-gated Ca^{2+} channels via activation of RhoA and its downstream effector, ROCK (79).

The present results indicate that the permeability of gap junctional channels of rat cardiac myocytes is rapidly affected (within minutes) by agents interfering with actin filament polymerization and, at longer term (a few hours), requires the activity of Rho small G-protein(s), most probably RhoA. Neither anchoring junctions nor most common Rho downstream kinase effectors (*e.g.* ROCK) appear to be involved in these effects; as Rho GTPases control the polymerization, branching, and bundling of actin, Rho might modulate the gating of gap junctional via the cell actin cytoskeleton. Junctional channels indeed do not operate as free floating entities in the plasma membrane but rather interact with specific cytoplasmic proteins (*e.g.* ZO-1) that link them to the actin cytoskeleton. Association with intracellular molecules is likely to be important for immobilization and clustering of the channels, for correct targeting of hemichannels to specific subcellular sites, for the ability of pores to funnel cell-to-cell ion and small molecules fluxes, and for modulation of the channel permeability by PKs, PPs, and other regulatory proteins. Thus the elucidation of interactions with intracellular proteins promises to reveal a great deal about the function, regulation, and cell biology of gap junctional channels. These structures mediate cell-cell communication in almost all tissues, but up to now, little has been known about their regulation by physiological stimuli. Acute exposures of ventricular myocytes to serotonin were recently seen (80)[3] to markedly enhance GJIC through activation of the RhoA downstream pathway. The present results provide further insight into the gating and regulation of junctional channels, confirm the important role of ZO-1 in the function of Cx43 gap junctions, and identify a new downstream target for the small G-protein RhoA. Such a switch process for Rho family proteins presents an additional layer of regulation in the transduction of biochemical signals to gap junctional intercellular communication.

Acknowledgments—We thank Drs. Patrice Boquet and Gilles Flatau (INSERM U452, Faculté de Médecine, Nice, France) who kindly provided CNF and Dr. Anne Cantereau (Institut de Physiologie et Biologie Cellulaires, Poitiers, France) for microscopy imaging expertise.

REFERENCES

1. Kanter, H. L., Saffitz, J. E., and Beyer, E. C. (1992) *Circ. Res.* **70,** 438–444
2. Sugiura, H., Toyama, J., Tsuboi, N., Kamiya, K., and Kodama, I. (1990) *Circ. Res.* **66,** 1095–1102
3. Verrecchia, F., Duthe, F., Duval, S., Duchatelle, I., Sarrouilhe, D., and Hervé, J. C. (1999) *J. Physiol.* **516,** 447–459
4. Duthe, F., Plaisance, I., Sarrouilhe, D., and Hervé, J. C. (2001) *Am. J. Physiol.* **281,** C1648–C1656
5. Wherlock, M., and Mellor, H. (2002) *J. Cell Sci.* **115,** 239–240
6. Etienne-Manneville, S., and Hall, A. (2002) *Nature* **420,** 629–635
7. Aoki, H., Izumo, S., and Sadoshima, J. (1998) *Circ. Res.* **82,** 666–676
8. Giepmans, B. N., and Moolenaar, W. H. (1998) *Curr. Biol.* **8,** 931–934
9. Toyofuku, T., Yabuki, M., Otsu, K., Kuzuya, T., Hori, M., and Tada, M.

[3] M. Derangeon, N. Bourmeyster, M. R. Popoff, J. A. Argibay, and J. C. Hervé, manuscript in preparation.

(1998) *J. Biol. Chem.* **273,** 12725–12731
10. Anderson, J. M. (1996) *Curr. Biol.* **6,** 382–384
11. Zhu, C., Barker, R. J., Hunter, A. W., Zhang, Y., Jourdan, J., and Gourdie, R. G. (2005) *Microsc. Microanal.* **11,** 244–248
12. Hunter, A. W., Barker, R. J., Zhu, C., and Gourdie, R. G. (2005) *Mol. Biol. Cell* **16,** 5686–5698
13. Barker, R. J., Price, R. L., and Gourdie, R. G. (2002) *Circ. Res.* **90,** 317–324
14. Plaisance, I., Duthe, F., Sarrouilhe, D., and Hervé, J. C. (2003) *Pfluegers Arch. Eur. J. Physiol.* **447,** 181–194
15. Bourmeyster, N., Stasia, M. J., Garin, J., Gagnon, J., Boquet, P., and Vignais, P. V. (1992) *Biochemistry* **31,** 12863–12869
16. Marvaud, J. C., Stiles, B. G., Chenal, A., Gillet, D., Gibert, M., Smith, L. A., and Popoff, M. R. (2002) *J. Biol. Chem.* **277,** 43659–43666
17. Wade, M. H., Trosko, J. E., and Schindler, M. (1986) *Science* **232,** 525–528
18. Délèze, J., Delage, B., Hentati, O., Verrecchia, F., and Hervé, J. C. (2001) *Methods Mol. Biol.* **154,** 313–327
19. Sezgin, M., and Sankur, B. (2004) *J. Electron. Imaging* **13,** 146–168
20. Laemmli, U. K. (1970) *Nature* **227,** 680–685
21. Zhao, Z. S., and Manser, E. (2005) *Biochem. J.* **386,** 201–214
22. Ishizaki, T., Uehata, M., Tamechika, I., Keel, J., Nonomura, K., Maekawa, M., and Narumiya, S. (2000) *Mol. Pharmacol.* **57,** 976–983
23. Huang, K. P., Itarte, E., Singh, T. J., and Akatsuka, A. (1982) *J. Biol. Chem.* **257,** 3236–3242
24. Sarrouilhe, D., Filhol, O., Leroy, D., Bonello, G., Baudry, M., Chambaz, E. M., and Cochet, C. (1998) *Biochim. Biophys. Acta* **1403,** 199–210
25. Yin, X., Jedrzejewski, P. T., and Jiang, J. X. (2000) *J. Biol. Chem.* **275,** 6850–6856
26. Zandomeni, R., and Weinmann, R. (1984) *J. Biol. Chem.* **259,** 14804–14811
27. Hervé, J. C., Bourmeyster, N., Sarrouilhe, D., and Duffy, H. S. (2007) *Prog. Biophys. Mol. Biol.* **94,** 29–65
28. Butkevich, E., Hulsmann, S., Wenzel, D., Shirao, T., Duden, R., and Majoul, I. (2004) *Curr. Biol.* **14,** 650–658
29. Hall, A. (1994) *Annu. Rev. Cell Biol.* **10,** 31–54
30. Grounds, H. R., Ng, D. C., and Bogoyevitch, M. A. (2005) *J. Cell. Biochem.* **95,** 529–542
31. Verrecchia, F., and Hervé, J. C. (1997) *Am. J. Physiol.* **272,** C875–C885
32. Nagy, J. I., Li, W. E., Roy, C., Doble, B. W., Gilchrist, J. S., Kardami, E., and Hertzberg, E. L. (1997) *Exp. Cell Res.* **236,** 127–136
33. Cooper, J. A. (1987) *J. Cell Biol.* **105,** 1473–1478
34. Dabiri, G. A., Turnacioglu, K. K., Sanger, J. M., and Sanger, J. W. (1997) *Proc. Natl. Acad. Sci. U. S. A.* **94,** 9493–9498
35. Thorburn, J., Xu, S., and Thorburn, A. (1997) *EMBO J.* **16,** 1888–1900
36. Luo, Y., and Radice, G. L. (2003) *J. Cell Sci.* **116,** 1471–1479
37. Hirose, M., Ishizaki, T., Watanabe, N., Uehata, M., Kranenburg, O., Moolenaar, W. H., Matsumura, F., Maekawa, M., Bito, H., and Narumiya, S. (1998) *J. Cell Biol.* **141,** 1625–1636
38. Uehata, M., Ishizaki, T., Satoh, H., Ono, T., Kawahara, T., Morishita, T., Tamakawa, H., Yamagami, K., Inui, J., Maekawa, M., and Narumiya, S. (1997) *Nature* **389,** 990–994
39. Fanning, A. S., Jameson, B., Jesaitis, L., and Anderson, J. M. (1998) *J. Biol. Chem.* **273,** 29745–29753.
40. Akoyev, V., and Takemoto, D. (2007) *Cell. Signal.* **19,** 958–967
41. Shumilina, E. V., Khaitlina, S. Y., Morachevskaya, E. A., and Negulyaev, Y. A. (2003) *FEBS Lett.* **547,** 27–31
42. Bishop, A. L., and Hall, A. (2000) *Biochem. J.* **348,** 241–255
43. Lampe, P. D., Qiu, Q., Meyer, R. A., TenBroek, E. M., Walseth, T. F., Starich, T. A., Grunenwald, H. L., and Johnson, R. G. (2001) *Am. J. Physiol.* **281,** C1211–C1222
44. Postma, F. R., Hengeveld, T., Alblas, J., Giepmans, B. N., Zondag, G. C., Jalink, K., and Moolenaar, W. H. (1998) *J. Cell Biol.* **140,** 1199–1209
45. Rouach, N., Pebay, A., Meme, W., Cordier, J., Ezan, P., Etienne, E., Giaume, C., and Tence, M. (2006) *Eur. J. Neurosci.* **23,** 1453–1464
46. Anderson, S. C., Stone, C., Tkach, L., and SundarRaj, N. (2002) *Investig. Ophthalmol. Vis. Sci.* **43,** 978–986
47. Czyz, J., Guan, K., Zeng, Q., and Wobus, A. M. (2005) *Int. J. Dev. Biol.* **49,** 33–41
48. Yatani, A., Irie, K., Otani, T., Abdellatif, M., and Wei, L. (2005) *Am. J. Physiol.* **288,** H650–H659
49. Hervé, J. C., and Sarrouilhe, D. (2006) *Prog. Biophys. Mol. Biol.* **90,** 225–248
50. Rajashree, R., Blunt, B. C., and Hofmann, P. A. (2005) *Am. J. Physiol.* **289,** H1736–1743
51. Verrecchia, F., and Hervé, J. C. (1997) *Pfluegers Arch. Eur. J. Physiol.* **434,** 113–116
52. Hopkins, A. M., Walsh, S. V., Verkade, P., Boquet, P., and Nusrat, A. (2003) *J. Cell Sci.* **116,** 725–742
53. Lerm, M., Pop, M., Fritz, G., Aktories, K., and Schmidt, G. (2002) *Infect. Immun.* **70,** 4053–4058
54. Tadvalkar, G., and Pinto da Silva, P. (1983) *J. Cell Biol.* **96,** 1279–1287
55. Wang, Y., and Rose, B. (1995) *J. Cell Sci.* **108,** 3501–3508
56. Yamane, Y., Shiga, H., Asou, H., and Ito, E. (2002) *Neuroscience* **112,** 593–603
57. McNicholas, C. M., Wang, W., Ho, K., Hebert, S. C., and Giebisch, G. (1994) *Proc. Natl. Acad. Sci. U. S. A.* **91,** 8077–8081
58. Kamouchi, M., Van Den Bremt, K., Eggermont, J., Droogmans, G., and Nilius, B. (1997) *J. Physiol.* **504,** 545–556
59. Hughes, B. A., and Takahira, M. (1998) *Am. J. Physiol.* **275,** C1372–C1383
60. Wang, Z., Eldstrom, J. R., Jantzi, J., Moore, E. D., and Fedida, D. (2004) *Am. J. Physiol.* **286,** H749–H759
61. Mironov, S. L., and Richter, D. W. (1999) *Eur. J. Neurosci.* **11,** 1831–1834
62. Lader, A. S., Kwiatkowski, D. J., and Cantiello, H. F. (1999) *Am. J. Physiol.* **277,** C1277–C1283
63. Kim, J. H., Rhee, P. L., and Kang, T. M. (2007) *Biochem. Biophys. Res. Commun.* **352,** 503–508
64. Theiss, C., and Meller, K. (2002) *Exp. Cell Res.* **281,** 197–204
65. Giepmans, B. N., Verlaan, I., Hengeveld, T., Janssen, H., Calafat, J., Falk, M. M., and Moolenaar, W. H. (2001) *Curr. Biol.* **11,** 1364–1368
66. Barker, R. J., Price, R. L., and Gourdie, R. G. (2001) *Cell Commun. Adhes.* **8,** 205–208
67. Laing, J. G., Manley-Markowski, R. N., Koval, M., Civitelli, R., and Steinberg, T. H. (2001) *J. Biol. Chem.* **276,** 23051–23055
68. Tamkun, M. M., O'Connell, K. M., and Rolig, A. S. (2007) *J. Cell Sci.* **120,** 2413–2423
69. Maass, K., Shibayama, J., Chase, S. E., Willecke, K., and Delmar, M. (2007) *Circ. Res.* **101,** 1283–1291
70. van Zeijl, L., Ponsioen, B., Giepmans, B. N., Ariaens, A., Postma, F. R., Varnai, P., Balla, T., Divecha, N., Jalink, K., and Moolenaar, W. H. (2007) *J. Cell Biol.* **177,** 881–891
71. Laing, J. G., Chou, B. C., and Steinberg, T. H. (2005) *J. Cell Sci.* **118,** 2167–2176
72. Laing, J. G., Saffitz, J. E., Steinberg, T. H., and Yamada, K. A. (2007) *Cardiovasc. Pathol.* **16,** 159–164
73. Hartsock, A., and Nelson, W. J. (2008) *Biochim. Biophys. Acta* **1778,** 660–669
74. Bruewer, M., Hopkins, A. M., Hobert, M. E., Nusrat, A., and Madara, J. L. (2004) *Am. J. Physiol.* **287,** C327–C335
75. Wheelock, M. J., and Johnson, K. R. (2003) *Curr. Opin. Cell Biol.* **15,** 509–514
76. Kostetskii, I., Li, J., Xiong, Y., Zhou, R., Ferrari, V. A., Patel, V. V., Molkentin, J. D., and Radice, G. L. (2005) *Circ. Res.* **96,** 346–354
77. Li, J., Patel, V. V., Kostetskii, I., Xiong, Y., Chu, A. F., Jacobson, J. T., Yu, C., Morley, G. E., Molkentin, J. D., and Radice, G. L. (2005) *Circ. Res.* **97,** 474–481
78. Matsuda, T., Fujio, Y., Nariai, T., Ito, T., Yamane, M., Takatani, T., Takahashi, K., and Azuma, J. (2006) *J. Mol. Cell. Cardiol.* **40,** 495–502
79. Piccoli, G., Rutishauser, U., and Brusés, J. L. (2004) *J. Neurosci.* **24,** 10918–10923
80. Derangeon, M., Defamie, N., Bourmeyster, N., Popoff, M., Boquet, P., Argibay, J. A., Sarrouilhe, D., and Hervé, J. C. (2007) *Arch. Mal. Coeur Vaiss.* **100,** 313